Available online at www.sciencedirect.com

ScienceDirect

Ceramics International 39 (2013) 9703–9707

CERAMICS INTERNATIONAL

www.elsevier.com/locate/ceramint

Short communication

Two-step freeze casting fabrication of hydroxyapatite porous scaffolds with bionic bone graded structure

Yufei Tang[a,*], Kang Zhao[a], Long Hu[a], Zixiang Wu[b]

[a]*School of Materials Science and Engineering, Xi'an University of Technology, Xi'an 710048, PR China*
[b]*Institute of Orthopaedics, Xi'jing Hospital, The Fourth Military Medical University, Xi'an 710032, PR China*

Received 22 January 2013; received in revised form 10 April 2013; accepted 10 April 2013
Available online 18 April 2013

Abstract

Hydroxyapatite (HA) porous scaffolds with bionic bone graded structure were fabricated by a two-step freeze casting. The phase, porosity, pore morphology, and compressive strength of the fabricated HA scaffolds were characterised. The HA scaffolds did not decompose after sintering at 1250 °C. The porosity of the inside and outside of the graded-porosity HA scaffolds was controlled by adjusting the initial HA content of the casting slurries. Cylindrical HA scaffolds with a radially aligned porosity gradient from the inside (highly porous) to the outside (less porous) were prepared, and a natural transition was found at the interface because partial melting–recrystallization occurred between the two sides. The compressive strength of the graded HA scaffolds depended on the porosity of the inner part. A compressive strength of 22.2 ± 4.1 MPa was achieved at an average porosity of 42.3% and outer thickness of about 2 mm.

Keywords: B. Porosity; C. Compressive strength; E. Biomedical applications; Two-step freeze casting

1. Introduction

Scaffolds have been used extensively in a variety of tissue engineering applications to provide a three-dimensional extracellular matrix analogue for in vivo and in vitro studies [1–3]. Such scaffolds can induce formation of bone from the surrounding tissue or act as a carrier or template for implanted bone cells and other agents [4,5]. To serve as a scaffold, the chosen materials should be biocompatible and osteoconductive, and have enough mechanical strength to provide structural support during bone growth and remodelling [6,7]. Hydroxyapatite (HA, $Ca_{10}(PO_4)_6(OH)_2$), a calcium phosphate that makes up most of the mineral phase of bone, is biocompatible and osteoconductive, and has excellent chemical and biological affinity with bony tissues [8,9]. The long-term biocompatibility of solid HA and its favourable interaction with soft tissue and bone have been thoroughly demonstrated [10–12]. Consequently, HA is widely accepted as a bioactive material for guided bone regeneration [13]. Biological studies and clinical practices have established that in addition to the requirements for compositional properties of the material, a porous structure is necessary [14,15].

In the shinbone, cylindrical channels of osteons are held together on the outside with a framework of highly open-spaced cancellous bone on the inside [16,17]. In general, highly porous scaffolds are reported to promote effective nutrient supply, metabolic waste removal, cell attachment, and intracellular signalling, but lead to low scaffold strength, while scaffolds with smaller porosity exhibit the opposite properties [18]. Thus, further studies examining the fabrication and characteristics of porous scaffolds that imitate the graded structure of bone are required. There are numerous reports on fabrication of pore graded ceramics, by methods including tape casting [19], centrifugal moulding [20], fibrous monolithic process [21], injected moulding [22], and freeze casting [23,24]. However, these techniques cannot be used to fabricate scaffolds with a naturally graded structure similar to that found in a bionic bone like the shinbone. The low mechanical properties of scaffolds with high porosity are also a limitation.

In the present study, we fabricated HA scaffolds with a graded structure similar to that of bionic bone using a two-step freeze drying method. The resulting cylindrical HA scaffolds had radially aligned porosity from the inside (highly porous) to

*Corresponding author. Tel./fax: +86 29 82312922.
E-mail address: yftang@xaut.edu.cn (Y. Tang).

0272-8842/$ - see front matter © 2013 Elsevier Ltd and Techna Group S.r.l. All rights reserved.
http://dx.doi.org/10.1016/j.ceramint.2013.04.038

the outside (more dense). The porosity range of the scaffold could be easily controlled by adjusting the HA content of the slurry. A natural transition was obtained at the interface because partial melting-recrystallization occurred between the two parts of each HA scaffold. The phases, porosity, and pore morphologies of the fabricated graded HA scaffolds were characterised, and their compressive strength was also investigated.

2. Experimental procedure

Commercially available HA powder (Fluke Co., UK) was used as the starting material, deionized water was used as the freezing medium, and polyvinyl alcohol (PVA; Yakuri Pure Chemicals Co. Ltd., Osaka, Japan) was used as a binder. A dispersant (polyacrylate sodium, PAAS; Sinopharm Chemical Reagent Co., Ltd, Shanghai, China) was used to stabilise the slurry.

Aqueous HA slurries with various HA contents were prepared by mixing the HA powder with 1 wt% dispersant and 0.5 wt% binder (relative to HA content) in deionized water. The prepared slurries (HA contents: 10, 20, 30 vol%) were poured into silicone rubber cylinders 10 mm in diameter and 40 mm in height. The cylinders were then placed on a pre-cooled plate in a freeze drier (VFD2000G, Boyikang Co. Ltd., Beijing, China). The samples were frozen by directional solidification at a temperature of −30 °C. The frozen samples acted as green bodies for the inner part of the graded structures, and were placed into the centre of polyethylene moulds 15 mm in diameter and 40 mm in height. HA slurry with 45 vol% HA content at 35 °C was poured into the space between the mould and the sample, and then the mould and its contents were again frozen in a freeze drier at −30 °C. Uniform porous HA scaffolds were also fabricated using various HA contents (10, 20, 30, 45 vol%). Both the HA porous scaffolds with bionic bone graded structure and the uniform porous HA scaffolds were dried to remove the ice and sintered at 1200–1300 °C in air for 3 h after complete solidification (shown in Fig. 1).

X-ray diffraction (XRD; Model 7000, Shimadzu Limited, Japan) was used to identify the phases present in the sintered samples. The pore morphology of the fabricated samples was characterised using scanning electron microscope (SEM, model JSM-6700F, JEOL, Japan) and a confocal laser scanning microscope (CLSM, model OLS 4000, OLYMPUS, Japan). The porosity of selected sections of the HA scaffolds was measured by Archimedes' principle. The compressive strength of the HA scaffolds was measured using a computer-servo-controlled materials testing machine (HT-2402-100KN, Hungta, Taiwan) operated at a rate of 0.2 mm/min. Five samples were tested to obtain average results for each preparation condition.

3. Results and discussion

Fig. 2 shows the XRD patterns of graded-structure HA scaffolds sintered at 1200, 1250, and 1300 °C. All peaks observed for the HA scaffolds sintered at 1200 and 1250 °C matched the JCPDS pattern 9-432 (hydroxyapatite), and showed no trace of decomposition. The diffraction peaks became narrower and sharper with increasing sintering temperature. The degrees of crystallisation of HA samples sintered at 1200 and 1250 °C were 51.48 and 59.36%, respectively, based on [25]. In contrast, the graded HA scaffold sintered at

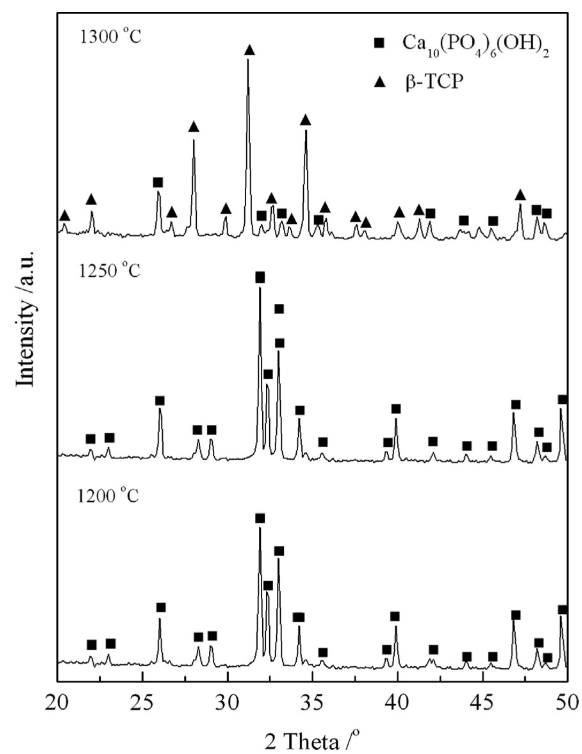

Fig. 2. XRD patterns of the HA scaffolds with graded structure sintered at different temperatures.

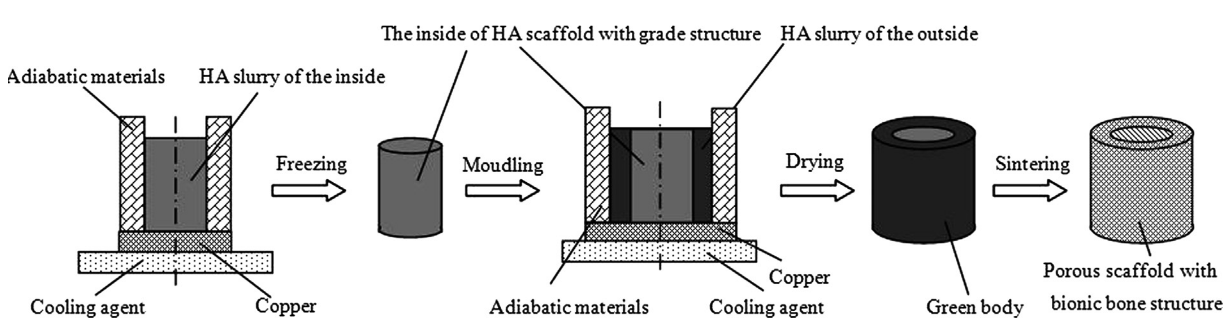

Fig. 1. Summary of the fabrication process.

1300 °C decomposed into β-tricalcium phosphate (β-TCP; reference pattern JCPDS 9-169). It has been reported that HA decomposes into tricalcium phosphate at temperatures above 1300 °C [26], and that this decomposition results in a sharp drop in strength and affects the osteoclastic resorption activity of HA. As expected, the freeze casting and sintering of the HA slurry did not affect the phase content of HA scaffolds sintered at 1250 °C.

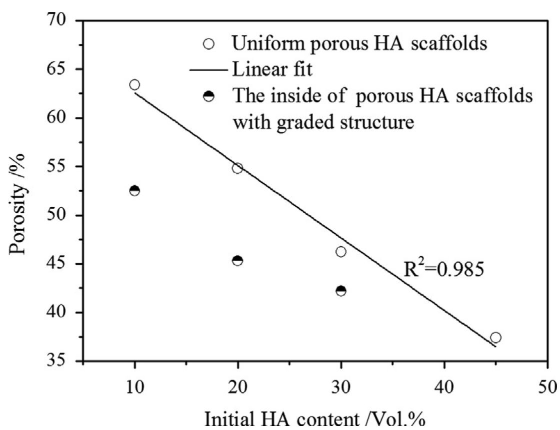

Fig. 3. Porosity of HA porous scaffolds with uniform and graded structures as a function of the initial HA content.

The apparent porosity of the HA scaffolds was measured using the Archimedes method. As the initial HA content was increased from 10 to 45 vol%, the porosity of the uniformly porous HA scaffolds linearly decreased from 63.4% to 37.4%, as shown in Fig. 3. The relationship between the porosity (P) and initial HA content (Φ) can be expressed as follows:

$$P = 70.0–0.745\Phi \tag{1}$$

This result indicates that the porosity of the inside and the outside of the graded-porosity HA scaffolds can be controlled by simply adjusting the initial HA content of the slurry. Moreover, the average porosity of the graded HA scaffold samples was between the porosities of their inner and outer parts. The average porosity of the graded-porosity scaffolds with outside initial HA content of 45 vol% decreased from 52.5% to 42.3% with inside initial HA content from 10 to 30 vol%.

Fig. 4 displays the morphologies of three HA scaffolds with graded structures. All scaffolds shown had an overall diameter of about 12 mm, outer thickness of about 2 mm, and outer porosity of 37.4%. The graded structure of the fabricated HA scaffolds was similar to that of a shinbone. The large porosity observed on the inside is expected to promote effective nutrient supply, metabolic waste removal, cell attachment, and intracellular signalling, while the lower porosity of the outside is expected to provide mechanical strength. Delamination was not observed in our graded HA scaffolds; instead,

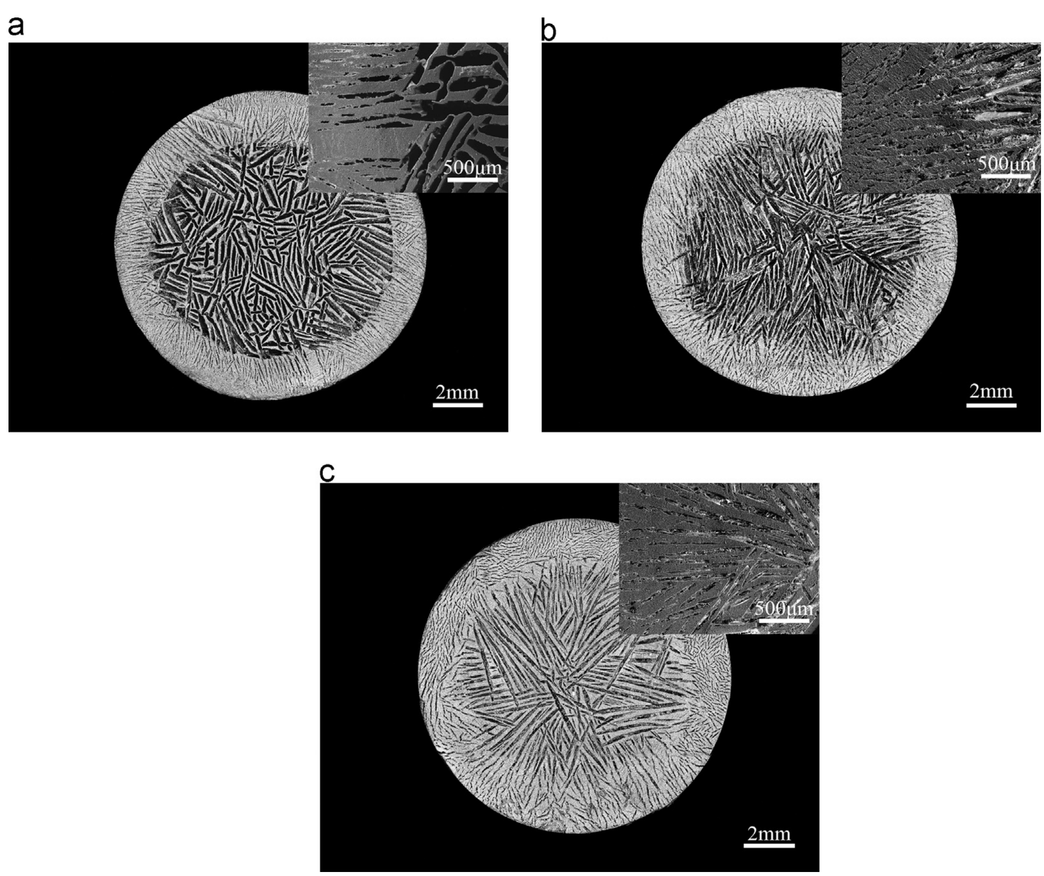

Fig. 4. Morphologies of HA porous scaffolds with graded structure: (a) average porosity 52.5%, inner initial HA content 10 vol%; (b) average porosity 45.3%, inner initial HA content 20 vol%; and (c) average porosity 46.2%, inner initial HA content 30 vol%.

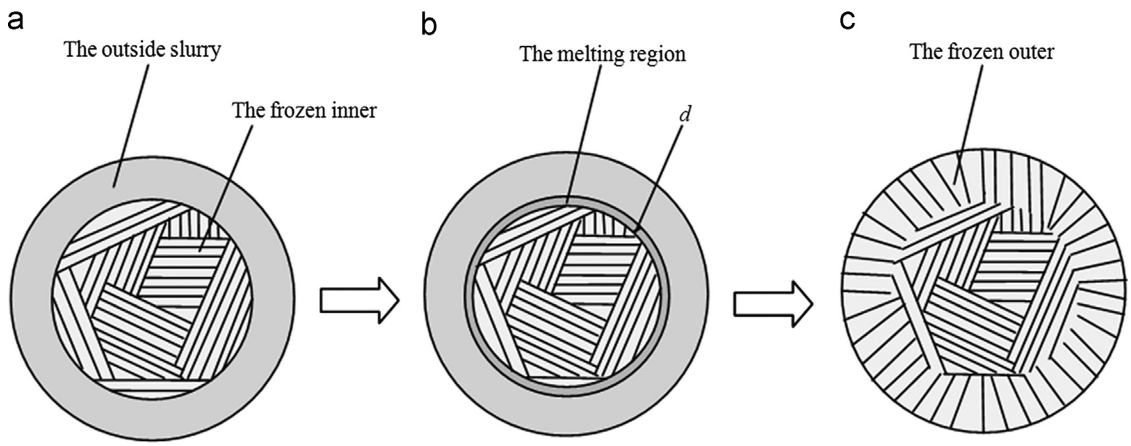

Fig. 5. Summary of melting–recrystallization that occurred at interface between frozen inside and outer slurry during second freeze casting process: (a) outer slurry was poured into space between mould and frozen inner part; (b) surface of frozen inner part melted; and (c) solvent of melt region recrystallised. Here, *d* is the size of the melting region.

good bonding at the interlayer between the inside and the outside could be seen in the enlarged images. Partial melting–recrystallization occurred at the interface between the frozen inside and the slurry of the outside during the second freeze casting process, as shown in Fig. 5. Fig. 5(a) shows the case where HA slurry with 45 vol% HA content at 35 °C had been poured into the space between the mould and the frozen inner part. The surface of the frozen inner part melted quickly after being surrounded by the outside slurry (Fig. 5(b)), and then blended into it. Here, *d* is the size of the melt region, and the factors influencing *d* were the temperature and physical properties of the slurries, and the ratio of the dimensions of the inside to outside. The solvent of the melt region and the outer slurry was frozen by the frozen inner part and the pre-cooled plate simultaneously. Ice crystals were distributed along the radial direction of the cylindrical samples, as shown in Fig. 5(c). A graded transition zone thus formed because the solvent was the same in the inside and outside, and the molten region was refrozen. In addition, a good graded transition was obtained, which decreased the porosity difference between the inside and the outside of the scaffold. A natural transition formed when the inner porosity was 46.2% and the outer porosity was 37.4%.

The compressive properties of HA scaffolds can be roughly estimated by considering their compressive strength normal to the direction of the applied load [27]. The compressive strengths of the uniform and graded-porosity HA scaffolds are plotted as a function of porosity in Fig. 6. The compressive strength of the uniform HA scaffolds decreased from 28.0 ± 4.2 to 4.2 ± 1.1 MPa with porosity increasing from 37.4% to 63.4%. Similarly, the compressive strength of the graded-porosity HA scaffolds also increased with decreasing average porosity. The compressive strengths of the three graded-porosity HA scaffolds were higher than those of uniform HA scaffolds of the same porosity. In uniaxial compression, the presence of a compliant inner part induces an axisymmetric buckling mode. It appeared that the aligned lamellar inner part of the present graded structures, which acted like a core/shell structure, increased their buckling resistance. The compressive strength of the graded-porosity HA scaffolds reached 22.2 ± 4.1 MPa at an average porosity of 42.3% and outer thickness of about 2 mm. Furthermore, the compressive strength of the graded-porosity HA scaffolds also depends on the size of the inner and outer parts, especially the thickness of the outside. This should be considered for precise modelling of compressive behaviour in the future.

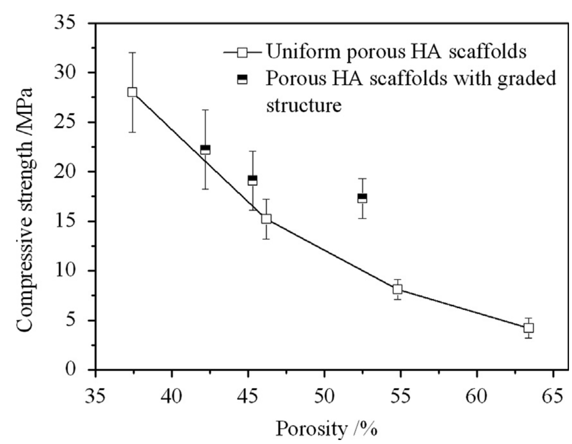

Fig. 6. Compressive strength of HA porous scaffolds with uniform and graded structures as a function of porosity.

4. Conclusions

In summary, a two-step freeze casting was used to produce porous hydroxyapatite (HA) scaffolds with a graded structure whose inside contained an aligned lamellar pore channel formed by directional solidification, with a surrounding relatively dense outside. A natural transition was found at the interface because partial melting–recrystallization occurred between the two parts. Furthermore, the porosities of the inside and outside of the scaffolds were controlled by adjusting the initial HA content used in the aqueous HA slurries. Their average porosity decreased from 52.5% to 42.3% with initial HA content of the inner part increasing from 10 to 30 vol%. The compressive strength of the graded-porosity HA scaffolds depended on the porosity of the inner part. A compressive strength of 22.2 ± 4.1 MPa was obtained at an average porosity of 42.3% and outer thickness of about 2 mm.

Acknowledgements

The authors would like to acknowledge the support from the National Natural Science Foundation of China (No. 51172179) and the Scientific Research Program Funded by Shaanxi Provincial Education Department (No. 2010JC18).

References

[1] J.A. Hubbell, in: Principles of Tissue Engineering, 2nd ed., Academic Press, San Diego, 2000.
[2] T.S. Karande, J.L. Ong, C.M. Agrawal, Diffusion in musculoskeletal tissue engineering scaffolds: design issues related to porosity, permeability, architecture, and nutrient mixing, Annals of Biomedical Engineering 32 (2004) 1728–1743.
[3] H. Shin, S. Jo, A.G. Mikos, Biomimetic materials for tissue engineering, Biomaterials 24 (2003) 4353–4364.
[4] A. Yokoyama, M. Gelinsky, T. Kawasaki, T. Kohgo1, U. König, W. Pompe, F. Watari, Biomimetic porous scaffolds with high elasticity made from mineralized collagen—an animal study, Journal of Biomedical Materials Research Part B: Applied Biomaterials 75 (2005) 464–472.
[5] M.W. Laschke, A. Strohe, M.D. Menger, M. Alini, D. Eglin, In vitro and in vivo evaluation of a novel nanosize hydroxyapatite particles/poly(esterurethane) composite scaffold for bone tissue engineering, Acta Biomaterialia 6 (2010) 2020–2027.
[6] K.J.L. Burg, S. Porterb, J.F. Kellam, Biomaterial developments for bone tissue engineering, Biomaterials 21 (2000) 2347–2359.
[7] S. Kim, S.S. Kim, S. Lee, S.E. Ahn, S.G. Wak, J. Song, B.S. Kim, H. M. Chung, In vivo bone formation from human embryonic stem cell-derived osteogenic cells in poly(D,L-lactic-co-glycolic acid)/hydroxyapatite composite scaffolds, Biomaterials 29 (2008) 1043–1053.
[8] A. Nakahira1, T. Murakami, T. Onoki, T. Hashida, K. Hosoi, Fabrication of porous hydroxyapatite using hydrothermal hot pressing and post-sintering, Journal of the American Ceramic Society 88 (2005) 1334–1336.
[9] L.M. Rodríguez-Lorenzo, M. Vallet-Regí, J.M.F. Ferreira, Fabrication of hydroxyapatite bodies by uniaxial pressing from a precipitated powder, Biomaterials 22 (2001) 583–588.
[10] H. Kusakabe, T. Sakamaki, K. Nihei, Y. Oyama, S. Yanagimoto, M. Ichimiya, J. Kimura, Y. Toyama, Osseointegration of a hydroxyapatite-coated multilayered mesh stem, Biomaterials 25 (2004) 2957–2969.
[11] S. Bose, S. Dasgupta, S. Tarafder, A. Bandyopadhyay, Microwave-processed nanocrystalline hydroxyapatite: simultaneous enhancement of mechanical and biological properties, Acta Biomaterialia 6 (2010) 3782–3790.
[12] T.M.G. Chu, D.G. Orton, S.J. Hollister, S.E. Feinberg, J.W. Halloran, Mechanical and in vivo performance of hydroxyapatite implants with controlled architectures, Biomaterials 33 (2002) 1283–1293.
[13] R. Emadi, F. Tavangarian, S.I.R. Esfahani, A. Sheikhhosseini, M. Kharaziha, Nanostructured forsterite coating strengthens porous hydroxyapatite for bone tissue engineering, Journal of the American Ceramic Society 93 (2010) 2679–2683.
[14] P. Sepulveda, F.S. Ortega, M.D.M. Innocentini, V.C. Pandolfelli, Properties of highly porous hydroxyapatite obtained by the gel casting of foams, Journal of the American Ceramic Society 83 (2000) 3021–3024.
[15] S. Deville, E. Saiz, R.K. Nalla, A.P. Tomsia, Freezing as a path to build complex composites, Science 311 (2006) 515–518.
[16] S. Deville, E. Saiz, A.P. Tomsia, Freeze casting of hydroxyapatite scaffolds for bone tissue engineering, Biomaterials 27 (2006) 5480–5489.
[17] S. Itoh, S. Nakamura, M. Nakamura, K. Shinomiya, K. Yamashita, Enhanced bone ingrowth into hydroxyapatite with interconnected pores by electrical polarization, Biomaterials 27 (2006) 5572–5579.
[18] A. Tampieri, G. Celotti, S. Sprio, A. Delcogliano, S. Franzese, Porosity-graded hydroxyapatite ceramics to replace natural bone, Biomaterials 22 (2001) 1365–1370.
[19] L. Ren, Y. Zeng, D. Jiang, Fabrication of gradient pore TiO_2 sheets by a novel freeze-tape-casting process, Journal of the American Ceramic Society 90 (2007) 3001–3004.
[20] C.H. Chen, K. Takita, S. Honda, H. Awaji, Fracture behavior of cylindrical porous alumina with pore gradient, Journal of the European Ceramic Society 25 (2005) 385–391.
[21] B. Lee, I.C. Kang, A.K. Gain, K. Kim, H. Song, Fabrication of pore-gradient Al_2O_3–ZrO_2 sintered bodies by fibrous monolithic process, Journal of the European Ceramic Society 26 (2006) 3525–3530.
[22] F. Zhang, J. Chang, J. Lu, K. Lin, C. Ning, Bioinspired structure of bioceramics for bone regeneration in load-bearing sites, Acta. Biomaterialia 3 (2007) 896–904.
[23] Y. Soon, K. Shin, Y. Koh, J. Lee, W. Choi, H. Kim, Fabrication and compressive strength of porous hydroxyapatite scaffolds with a functionally graded core/shell structure, Journal of the European Ceramic Society 31 (2011) 13–18.
[24] A. Macchetta, I.G. Turner, C.R. Bowen, Fabrication of HA/TCP scaffolds with a graded and porous structure using a camphene-based freeze-casting method, Acta Biomaterialia 5 (2009) 1319–1327.
[25] Y.X. Pang, X. Bao, Influence of temperature, ripening time and calcination on the morphology and crystallinity of hydroxyapatite nanoparticle, Journal of the European Ceramic Society 23 (2003) 1697–1704.
[26] T.K. Chaki, P.E. Wang, Densification and strengthening of silver-reinforced hydroxyapatite-matrix composite prepared by sintering, Journal of Materials Science: Materials in Medicine 5 (1994) 533–542.
[27] A. Hattiangadi, A. Bandyopadhyay, Strength degradation of nonrandom porous ceramic structures under uniaxial compressive loading, Journal of the American Ceramic Society 83 (2000) 2730–2736.